Electron Linear Accelerator Based on $\mathbf{V}_p \times \mathbf{B}$ Acceleration Scheme

Y. Nishida, N. Yugami, H. Onihashi,[a] T. Taura, and K. Otsuka

Department of Electrical and Electronic Engineering, Utsunomiya University, Utsunomiya, Tochigi 321, Japan

(Received 16 July 1990)

A new type of electron linear accelerator realized in a vacuum system, based on the $\mathbf{V}_p \times \mathbf{B}$ acceleration scheme observed originally in plasma, has been demonstrated. The present system has a static magnetic field applied vertically to the wave propagation direction, and the particles are accelerated along the wave front at constant phase with respect to the wave. In this scheme, a greater acceleration rate than that of conventional linear accelerators has been observed. The acceleration rate is also larger than that expected from the simple theoretical model presented so far.

PACS numbers: 41.80.−y, 29.15.Dt, 52.75.Di

The recent particle accelerators demand new acceleration principles that can create a high field gradient, because the popularly known acceleration principles cannot reach a high enough field gradient, and so require a tremendously large apparatus in order to obtain fully accelerated high-energy particles. Several new concepts have been proposed for making a breakthrough in this present dilemma,[1-6] one of which is a $\mathbf{V}_p \times \mathbf{B}$ acceleration scheme[3,4,7] (or a surfatron[6]). In this accelerator, the wave which traps particles in a wave trough travels across a static magnetic field, and the particles can be accelerated along the wave front[3-6,8] keeping a constant phase in the wave trough.

In this paper, we show the first experimental demonstration of an electron linear accelerator realized in a vacuum system,[7] which is based on the $\mathbf{V}_p \times \mathbf{B}$ acceleration scheme, and the results show a greater acceleration rate than that of conventional electron linear accelerators.

A charged particle in the $\mathbf{V}_p \times \mathbf{B}$ scheme is trapped in an electromagnetic wave (TM mode, which has a longitudinal component of the wave electric field) with a phase velocity V_p in the z direction immersed in a static magnetic field B in the x direction (see Fig. 1 in Ref. 7). The Lorentz force $F_y = qV_pB$ accelerates the particle in the y direction, where q is an electric charge. The velocity V_y thus produced creates a Lorentz force $F_z = qV_yB$ in the $-z$ direction to keep the particle at the position of maximum field E_m, the wave electric field. Although the Lorentz force cannot directly increase the particle energy, the particle can gain energy from the wave electric field. If the condition

$$E_m > \gamma_p Bc > \gamma_p BV_y \tag{1}$$

is satisfied, the particles kept at the equilibrium point in the wave are never released from the wave field. The energy gain in steady state for a unit length is the same as that originally obtained on the surfatron,[6]

$$\frac{d\gamma}{dy} = \gamma_p \frac{\gamma_p \omega_c V_p}{c^2}, \tag{2}$$

$$\frac{d\gamma}{dz} = \gamma_p \frac{\omega_c^2 z}{c^2}\left[1 + \frac{\omega_c^2 z^2}{c^2}\right]^{-1/2}, \tag{3}$$

where $\gamma_p = [1-(V_p/c)^2]^{-1/2}$, $\gamma = [1-(V/c)^2]^{-1/2}$, and ω_c is the electron cyclotron frequency measured with a rest mass. It is seen that $d\gamma/dy$ is γ_p times larger than $d\gamma/dz$, if $V_p \simeq c$ and $\omega_c^2 z^2/c^2 \gg 1$ are taken into account, that is, the acceleration rate in the y direction is more efficient than in the z direction for $\gamma_p > 1$. Therefore, $L_y/L_z = (\gamma_p^2 - 1)^{-1/2} \simeq 1/\gamma_p$ $(\gamma_p \gg 1)$, where L_y and L_z are, respectively, the length in the y and z directions necessary for acceleration to yield the same amount of energy.

The experimental apparatus shown in Fig. 1 is designed for the purpose of a proof of the principle of the $\mathbf{V}_p \times \mathbf{B}$ acceleration scheme in a vacuum system.[7,9] The electron gun for beam injection has a maximum energy of 100 keV with a maximum beam current of 1.5 mA. A precise description of the system has been given elsewhere[9] (see also Fig. 1). The acceleration section has a slow-wave structure of TM mode, which is a parallel-fin electrode type with 50 cm length in the wave propagation direction, and is designed so that the phase velocity is $0.46c$ (corresponding energy of 66 keV). The rf source is a magnetron of 2.45 GHz with a typical pulse width of 5 μsec in repetition at 10 Hz. The maximum power is 3.5 kW.

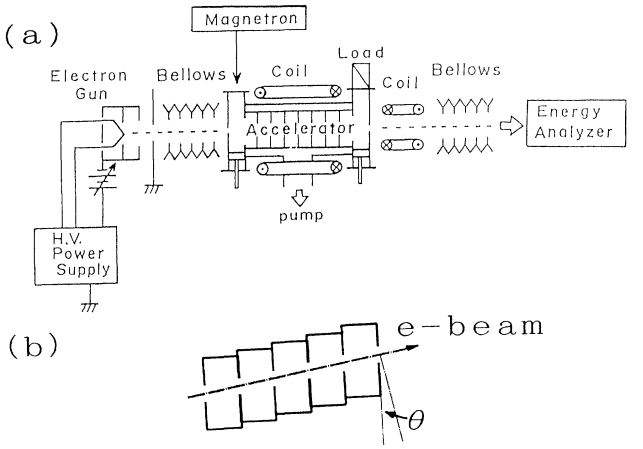

FIG. 1. (a) Experimental apparatus for the proof of the principle of the electron linear accelerator based on the $\mathbf{V}_p \times \mathbf{B}$ acceleration scheme, and (b) an example of the tilted-fin-type slow-wave structure for a relativistic beam.

A vertical magnetic field in the x direction is produced by a pair of saddle-shaped coils with uniform length of 32 cm (less than 3% uniformity; 40 cm for 5%) in the z direction and +5 cm (less than 3%) in the y direction. A typical strength of the applied static magnetic field is about 3 G which is determined by the trapping condition Eq. (1). An electron beam accelerated in the slow-wave structure is analyzed by an energy analyzer with a resolution of less than 0.5 keV. The present accelerator can be operated as either a conventional linear accelerator without static magnetic field or a $\mathbf{V}_p \times \mathbf{B}$ accelerator with vertical magnetic field, without any serious change in the machine. All the experiments were performed in steady state, and the data were sampled and averaged over a long enough time duration by using a boxcar averager with a gate width of typically 50 nsec.

Typical examples of the observed energy spectrum are shown in Fig. 2, where (a) the incident beam energy is the parameter, at constant magnetic field of $B=2$ G, and (b) the static magnetic-field strength is the parameter, at constant incident beam energy of 48 keV. A nonaccelerated incident-beam component is seen in the lower-energy region as well as an accelerated high-energy part in Fig. 2(a). When the static magnetic field is increased, two peaks, a high-energy one and a lower one, appear clearly at typically $B \simeq 1.5$ G as shown in Fig. 2(b). The lower-energy peak corresponds, typically, to about 40 keV, decelerated from the injected component of 48 keV. For further increase of the magnetic field ($B > 3$ G), the high-energy component decelerates to merge with the lower one, and acceleration no longer occurs as the trapping condition for the particle, Eq. (1), is violated. The energy spread of the accelerated beam around $B=0.5$–2.0 G is narrower in the case of a vertical magnetic field than in the case without it. This fact shows that the particles can be bunched stably into a certain phase of the wave, where the field strength is maximum theoretically, when the vertical magnetic field exists. The energy increment measured relative to the incident beam energy $\Delta\varepsilon$ as a function of the static magnetic-field strength is shown in Fig. 3, which is obtained from Fig. 2(b). Note that the machine is working in steady state and the error bars of $\Delta\varepsilon$ are within the size of the data symbols. The particle energy reaches the maximum value, 15 keV, around $B=2$ G, and then the acceleration rate decreases. Up to $B \lesssim 2$ G, the energy increment $\Delta\varepsilon$ is proportional to B^2, i.e., $\Delta\varepsilon - \Delta\varepsilon(B=0) \propto B^2$. The trapping condition Eq. (1) can be checked by using the present parameters, and the maximum field strength for particle trapping is obtained to be about 2.0 G, in good agreement with the experimental results. After the breaking of the trapping condition, Eq. (1), the energy quickly decreases with an increase of the magnetic field.

The energy increment $\Delta\varepsilon$ versus the incident beam energy with a microwave power of 2.3 kW was observed after a minor change of the facilities, for possible measurement of particles bent more in the y-z plane, and the results are shown in Fig. 4, in which "0 G" again stands for the case of a conventional linear accelerator. When the incident beam energy is 48 keV, for example, the observed electron energy is 56 keV ($\Delta\varepsilon=8$ keV) with a static magnetic field of 3 G ($\mathbf{V}_p \times \mathbf{B}$ accelerator), while in the conventional accelerator the electron energy reaches 52.0 keV, and $\Delta\varepsilon=4.0$ keV. From this we can obtain an average field strength of about 8 kV/m. Here, the calculated maximum field strength for trapping in this case is about 2.2 G, even smaller than the observed value. When the energy increment $\Delta\varepsilon$ is observed as a function of the applied static magnetic field, the $\mathbf{V}_p \times \mathbf{B}$ accelera-

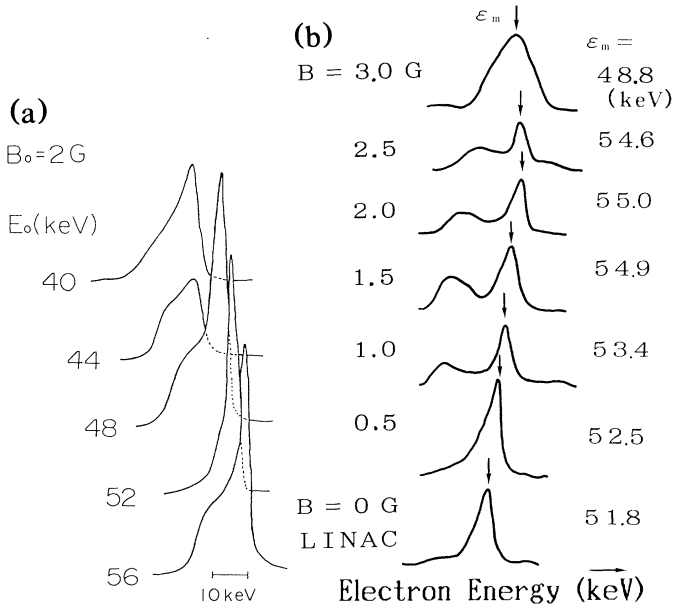

FIG. 2. Typical electron energy spectrum (a) observed as a function of the incident electron energy at a constant static magnetic field $B_0=2$ G and microwave power $P=1.3$ kW, and (b) observed as a function of the static magnetic field at constant incident beam energy of $E_0=48$ keV and $P=2.5$ kW. ε_m indicates the energy as is observed.

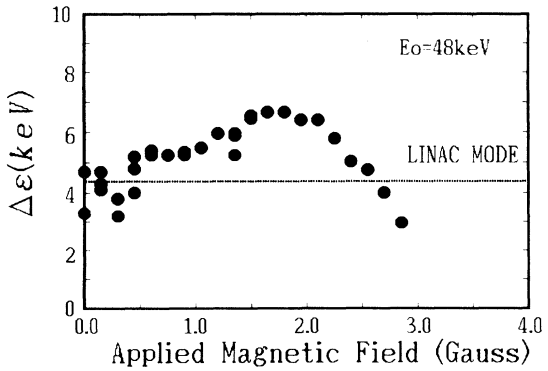

FIG. 3. Energy increment $\Delta\varepsilon$ as a function of the static magnetic-field density, from Fig. 2(b).

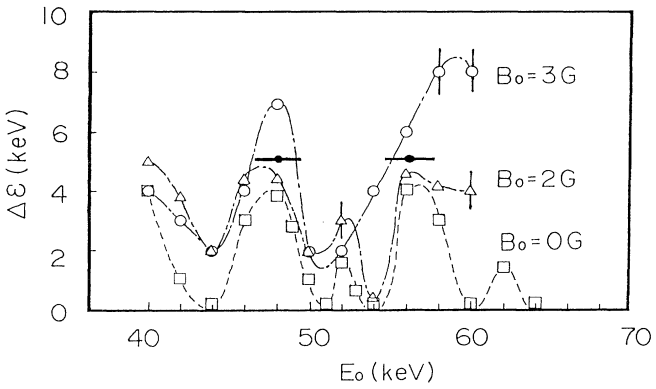

FIG. 4. Energy increment $\Delta\varepsilon$ as a function of the incident electron energy E_0. □, $B_0=0$ G (conventional electron linear accelerator); △, $B_0=2$ G; ○, $B_0=3$ G; and ● calculated values around $E_0=48$ and 56 keV at $B_0=3$ G. Microwave power is about 2.5 kW.

tor achieves a higher energy than the conventional linear accelerator, showing an efficient acceleration rate [see also Figs. 2(b) and 3]. The expected increment of the electron energy was calculated from Eqs. (2) and (3) for the case of $B=3.0$ G around $E_0=48$ and 56 keV, and the results are shown by solid circles in Fig. 4. When the acceleration rates are calculated from Eqs. (2) and (3), we cannot use the assumption that $V_p \lesssim c$ ($\gamma_p \gg 1$), but instead the complete Eqs. (2) and (3). Figure 4 shows that the calculated values are smaller than the experimental results; the reasons for the discrepancies are under consideration. The difference between the maximum energy increment $\Delta\varepsilon$ seen in Figs. 3 and 4 may come from the fact that the microwave power is higher in Fig. 3 (about 3.2 kW) than in Fig. 4 (less than about 2.5 kW). Unfortunately, the dependence of the maximum particle energy on the microwave power has not been observed because of the lack of a variable power tuning system, except for only two points.

It is clearly seen from the experimental results shown in Figs. 2 and 3 that the $\mathbf{V}_p \times \mathbf{B}$ acceleration scheme gives a more effective acceleration rate than the conventional linear accelerator. The observed value of the phase velocity was smaller than that expected from the design values because of the homemade, and not very accurate, slow-wave structure. However, there was no serious problem in achieving the present phenomena, although several submodes were observed as seen in Fig. 4.

When the present machine is used as a conventional linear accelerator without a static magnetic field, the electron beam traverses the region with maximum field strength in the slow-wave structure. In other words, the maximum particle energy could be reached in the conventional mode. In the case of the $\mathbf{V}_p \times \mathbf{B}$ accelerator, however, the orbit of an electron beam bends slightly because of the slow beam velocity ($0.46c$) and the electron cannot travel in the area with maximum field strength, resulting in a weaker acceleration rate. Numerical calculation of the field strength in the y direction shows about 5% weaker values on average with respect to the maximum field strength at the center, and we conclude that the variation of the wave field strength in the y direction does not seriously change the particle energy. It should be mentioned that, in the present machine, the electron beam is *decelerated* in the front half of the whole machine length as the injected beam should bend in the y-z plane because of the slow wave phase velocity, and that the latter half of the machine works as the $\mathbf{V}_p \times \mathbf{B}$ *accelerator*. This is only because we used the same machine as both the conventional linear accelerator and the $\mathbf{V}_p \times \mathbf{B}$ accelerator without having to change any facilities at all. Nevertheless, we have observed an electron energy more than 80% higher in the $\mathbf{V}_p \times \mathbf{B}$ scheme. This fact requires further theoretical work.

As discussed by Neuffer,[10] the particles trapped at the equilibrium point $\sin\phi_1 = \gamma_p Bc/E_0$ in the wave frame, where ϕ_1 is the equilibrium phase in the wave frame, can emit no seriously strong synchrotron radiation, and the radiation rate is the same as in the conventional linac. In the early stage of the acceleration, however, the particle trace changes as $y \simeq \frac{1}{2}\omega_c V_p t^2/\gamma_p$ for $\omega_c t \ll 1$, at $V_p \simeq c$, the synchrotron radiation could be expected, because many of the particles are not necessarily in the equilibrium state. After sufficient acceleration ($\omega_c t \gg 1$; in the present machine $t \gtrsim 20$ nsec is required), the particle trace is given by $y = ct/\gamma_p$ in the wave frame.[8] Therefore, in the later stage where the particle reaches sufficiently high energy, the particle travels exactly straight in two-dimensional space and no extra radiation is expected. When we look at the parameters in the present experiment, the time required for the particle passing through the whole machine is about 3.6 nsec. Therefore, not all of the particles are necessarily bunched into the equilibrium position, and the particle orbit is bent. The theory, on the other hand, is deduced for the final steady state, and the transient phenomena, which could be expected to occur in the early stage, are not taken into consideration for interpreting the present results. The particles in the transient stage oscillate around an equilibrium point, specifically in the z direction, and the high-energy phase of the particles in the wave could be observed in the results. The bouncing period of the particles around the final equilibrium point in the wave grows with the acceleration time as $t^{1/2}$ and the bouncing amplitude damps out in proportion to $t^{-1/4}$. Therefore, the particles will go to the steady equilibrium point in a short period. Precise investigations on this phenomenon are underway and will be presented elsewhere.

As a realistic numerical example of the linac based on the present scheme, we can employ $B=235$ G for a maximum wave field $E_m=50$ MV/m, and we need a machine length $L_z=230$ m and $L_y=32.6$ m in order to obtain 11-GeV electrons accelerated from 3.6 MeV ($\gamma_p=7.0$).

Here, it should be mentioned that the particles in the present scheme travel in two dimensions (y-z plane). The width L_y in the transverse direction seems to be fairly large. In the actual scheme, however, the accelerator width could be made narrow enough, comparable to the conventional linear accelerator, by employing a tilted-fin-type electrode for a delay circuit[7] such as schematically shown in Fig. 1(b), in which the tilting angle θ is defined as indicated. If the phase velocity is close to the speed of light, the angle θ is known to get smaller as $\sin\theta \simeq 1/\gamma_p$. Here, it is also recognized that the particles with an initial energy of 3.6 MeV may radiate synchrotron radiation with a power of $\Delta W \simeq 4\times 10^{-6}$ eV, and in the final stage with the particle energy 11 GeV, $\Delta W \simeq 1\times 10^{5}$ eV is expected. Therefore, there may be no serious energy loss from this process in the present scheme.

It should be mentioned that in the conventional linac the maximum field strength for the acceleration could be limited by, say, a breakdown between the electrodes of the slow-wave structure. In the present machine this condition may also exist, but the acceleration rate in the transverse direction is γ_p ($\gg 1$) times more efficient in the present system, and more energetic particles compared with the ones accelerated by the conventional method are expected, if the same field strength is employed. In the present slow-wave structure, there exists a radial electric-field component E_x parallel to the static magnetic field, except for the center-axis area. Therefore, in the off-axis area, this field works to pull the particles out into the fin electrodes. To prevent this effect in a structure such as the present square type, one possibility is to add a weak static electric field with opposite polarity to the wave electric field. The stable acceleration phase exists within a quarter period of the wave, and the particles should be injected only into this phase for a high-quality-beam accelerator; this is different from the present simple system, in which we used a dc electron beam.

In conclusion, a new electron linear accelerator based on the $\mathbf{V}_p\times\mathbf{B}$ acceleration scheme has been demonstrated for the first time in a vacuum system. The experimental results show that the $\mathbf{V}_p\times\mathbf{B}$ accelerator boosts the particle energy more effectively than the conventional linear accelerator. We need more precise theoretical works to interpret the complete set of experimental results.

The authors are indebted to Professor R. Sugihara and Dr. S. Takeuchi for discussions. A part of the present work has been supported by the Grant-in-Aid for Scientific Research from the Ministry of Education, Science and Culture, Japan.

---

[a]Present address: Toshiba Co. Ltd., Ohtawara, Tochigi 329-26, Japan.

[1]T. Tajima and J. M. Dawson, Phys. Rev. Lett. **43**, 267–270 (1979).

[2]P. Chen, J. M. Dawson, R. W. Huff, and T. Katsouleas, Phys. Rev. Lett. **54**, 693–696 (1985).

[3]R. Sugihara and Y. Mizuno, J. Phys. Soc. Jpn. **47**, 1290–1295 (1979).

[4]Y. Nishida, M. Yoshizumi, and R. Sugihara, in *Proceedings of the Thirteenth Annual Anomalous Absorption Conference,* Banff, Alberta, Canada, 5–10 June 1983 (unpublished), p. F7; Phys. Lett. **105A**, 300–302 (1984); Y. Nishida, M. Yoshizumi, and R. Sugihara, Phys. Fluids **28**, 1574–1576 (1985).

[5]C. Joshi and T. Katsouleas, in *Laser Acceleration of Particles,* edited by C. Joshi and T. C. Katsouleas, AIP Conf. Proc. No. 130 (AIP, New York, 1985).

[6]T. Katsouleas and J. M. Dawson, Phys. Rev. Lett. **51**, 392–395 (1983).

[7]Y. Nishida and R. Sugihara, in *Laser Interaction and Related Plasma Phenomena,* edited by H. Hora and G. Miley (Plenum, New York, 1986), Vol. 7, pp. 803–809.

[8]Y. Nishida, in Proceedings of the Nineteenth International Conference on Phenomena in Ionized Gases, 10–14 July 1989, Belgrades, Yugoslavia, edited by Vida J. Zigman (to be published).

[9]Y. Nishida and H. Onihashi, in *Proceedings of the Sixth Symposium on Accelerator Science and Technology, Tokyo* (IONICS, Tokyo, 1987), p. 183.

[10]D. V. Neuffer, Phys. Rev. Lett. **53**, 1026 (1984).